

Targeting a Multidrug-Resistant Pathogen: first generation antagonists of *Burkholderia cenocepacia*'s BC2L-C lectin

Rafael Bermeo, Kanhaya Lal, Davide Ruggeri, Daniele Lanaro, Sarah Mazzotta, Francesca Vasile, Anne Imberty, Laura Belvisi, Annabelle Varrot, Anna Bernardi

ABSTRACT: Multi-drug resistant (MDR) pathogens such as *Burkholderia cenocepacia* have become a hazard in the context of healthcare-associated infections, especially for patients admitted with cystic fibrosis or immuno-compromising conditions. As other opportunistic Gram-negative bacteria, this pathogen establishes virulence and biofilms through lectin-mediated adhesion. In particular, the *superlectin* BC2L-C is believed to cross-link human epithelial cells to *B. cenocepacia* during pulmonary infections. We aimed to obtain glycomimetic antagonists able to inhibit the interaction between the *N*-terminal domain of BC2L-C (BC2L-C–Nt) and its target fucosylated human oligosaccharides. In a previous study, we identified by fragment virtual screening and validated a small set of molecular fragments that bind BC2L-C–Nt in the vicinity of the fucose binding site. Here we report the rational design and synthesis of bifunctional *C*- or *N*-fucosides, generated by connecting these fragments to a fucoside core using a panel of rationally selected linkers. A modular route starting from two key fucoside intermediates was implemented for the synthesis, followed by evaluation of the new compounds as BC2L-C–Nt ligands with a range of techniques (SPR, ITC, STD-NMR, DSC and X-ray crystallography). This study resulted in a hit molecule with an order of magnitude gain over the starting methyl fucoside and in two crystal structures of antagonist/lectin complexes.

▪ INTRODUCTION

The rising threat of anti-microbial resistance (AMR) poses a particular hazard to hospital-bound patients: opportunistic infections from multi-drug-resistant (MDR) ‘superbugs’ prey on the weakened systems of patients suffering from immuno-compromising conditions, cystic fibrosis, and other debilitating illnesses. These healthcare-associated infections become ever more worrisome in the current global context and have triggered action plans worldwide.^{1,2}

Among the MDR pathogens, *Pseudomonas aeruginosa* and members of the *Burkholderia cepacia* complex (BCC) are notorious lung pathogens: they periodically surface in hospitals and hold the ability to form biofilms.^{3,4} Particularly hazardous for cystic fibrosis patients, pulmonary infections

by BCC bacteria may lead to “cepacia syndrome”, a rapid decline of respiratory function leading to sepsis and high mortality rate. The main pathogen responsible for cepacia syndrome is *Burkholderia cenocepacia*, a globally spread bacterium.⁴ As for *P. aeruginosa* and many other pathogens, *B. cenocepacia*'s ability to colonize and invade host tissues strictly depends on bacterial adhesion,⁵ which is often mediated by carbohydrate/protein interactions. Indeed, human oligosaccharide antigens, particularly the histo-blood groups, are consistently targeted by microbial lectins that represent virulence factors in the context of infection.⁶ Disrupting bacterial lectins binding to host glycans prevents microbial adhesion, hinders the infective process at its inception and leads to better clinical outcomes. This strategy, known as anti-adhesion therapy (AAT) is viable to complement and complete antibiotic therapy. AAT combats infection without killing the pathogen: compared to antibiotics, the lack of selective pressure is expected to reduce the appearance of mutations leading to AAT-resistant strains.^{7,8}

Glycomimetics have proven their worth for AAT as reliable disruptors of carbohydrate/lectin interactions. Designed to emulate carbohydrate structure and/or function, glycomimetics display improved physicochemical and pharmacokinetic properties (improved oral bioavailability, adjusted polarity and metabolic stability). Such molecules have successfully been used to target both microbial and human carbohydrate-binding proteins known to be vectors of virulence.^{9–12} Nonetheless, the design of glycomimetics directed against specific lectin targets remains a challenging problem, owing to the intrinsically low affinity of carbohydrate-protein interactions and to the structural characteristics of lectin binding sites that are not well-suited for most of the classical tools of structure-based molecular design.^{12,13} Here we describe the rational design, synthesis and activity evaluation of fucose-based glycomimetic ligands targeted against a recently described virulence factor of *B. cenocepacia*, the BC2L-C lectin.

BC2L-C was discovered through a genetic screening in *B. cenocepacia* for genes resembling the *lecB* gene of *P. aeruginosa*. In the extensively studied *P. aeruginosa*, LecB, encoded by the *lecB* gene, is a fucose specific lectin involved in bacterial adhesion and biofilm formation. It represents a virulence factor and a major determinant for lung infection.^{14–18} In *B. cenocepacia*, the screening returned a lectin family composed of four proteins BC2L-A-D, all containing a LecB-like C-terminal dimeric domain,^{19–21} BC2L-C was also found to contain an N-terminal trimeric domain, which features specific millimolar affinity for L-fucose and high micromolar affinity for fucosylated histo-blood oligosaccharides.²² Thus BC2L-C presents a double carbohydrate specificity, maintained through a hexameric assembly, which makes it a *superlectin*, hypothesized to crosslink cells by simultaneously binding bacterial mannosides in its C-terminal domain and human fucosides in the N-terminal domain.^{20,22}

The inhibition of BC2L-C and of its crosslinking capacity provides a clear opportunity to employ AAT to reduce the effects of *B. cenocepacia* infections. Since its C-terminal domain is related to LecB, which has been extensively targeted and studied,^{16-19,23} we chose to focus on the fucose-specific N-terminal domain (BC2L-C-Nt). Our initial work focused on characterizing the recombinant version of BC2L-C-Nt (rBC2L-CN), its carbohydrate binding site and its interaction with histo-blood group ligands H-type 1 and H-type 3 (Globo H).²⁴ Thanks to the structural data obtained, computational work allowed mapping the protein surface for potential ligandable sites. A fragment screening campaign validated by X-ray data provided a small library of molecular entities predicted to bind near the fucose-occupied binding site.²⁵ Based on these results, we now have rationally designed and synthesized a panel of first-generation BC2L-C-Nt glycomimetic ligands. We probed these molecules against their target through different biophysical techniques, and identified a hit compound. The leading fucoside glycomimetic showed an affinity increase of nearly one order of magnitude over the starting monosaccharide α -Me-L-Fucoside (α MeFuc). Furthermore, we obtained the crystal structures of BC2L-C-Nt in complex with the lead structure and with a second ligand.

▪ RESULTS AND DISCUSSION

Design of Fucoside BC2L-C-Nt Antagonists

We previously described the *in silico* study of BC2L-C-Nt leading to the detection of a ‘ligandable’ site, which consists in a crevice near the lectin’s fucose-binding site (**Figure 1A**). Both sites are located at the interface of two protomers in the BC2L-C-Nt trimer. Virtual screening of a fragment library in the BC2L-C-Nt complex with α -methylselenyl-fucoside (PDB 2WQ4) resulted in the selection of molecular fragments predicted to bind the vicinal site, which were validated by biophysical techniques.²⁵ Selected fragments are used here for the design of new bifunctional molecules, generated by connecting the fragment to a fucoside core. Generally, the fragments employed are constituted by an aromatic moiety, predicted to interact in the newly detected binding site through edge-to-face interactions with residue Tyr58. Additionally, some fragments contain a terminal amino group, predicted by the virtual screening to participate in an ionic or polar interaction with residue Asp70 at the bottom of the crevice (**Figure 1A**). The structures of the fragment moieties are shown in **Table 1**. Additional comments on their structure and selection are collected in the Supporting information (Section 2.1, **Figure S1**).

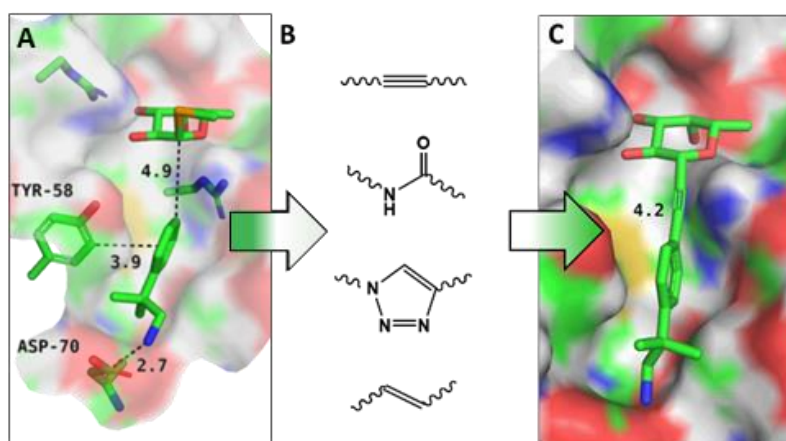


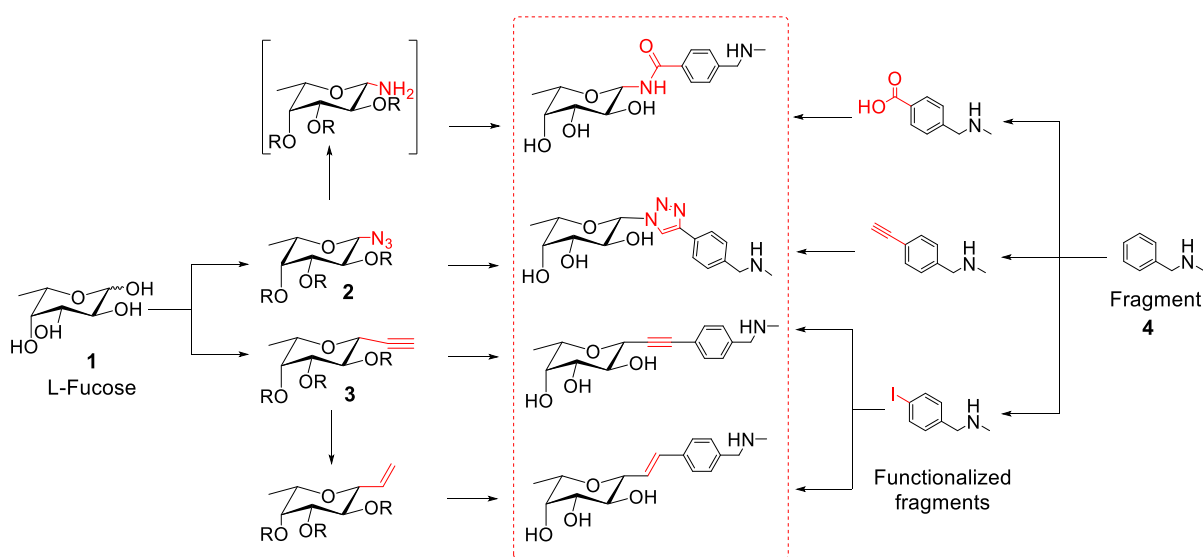
Figure 1. Ligand design strategy: (A) Example of a fragment screening hit, (B) Chemical linkages considered, (C) Example of a BC2L-C-Nt antagonist. Distances (Å, black) from anomeric carbon to closest fragment atom.

Figure 1 describes the ligand design strategy: (A) the hits from fragment screening were found in close proximity (4-6 Å) to the fucoside's anomeric position, in the direction of the β -substituent. This provided a clear synthetic strategy involving functionalization of the anomeric carbon, which was selected as the linking point. (B) A panel of connectors were considered to link the fragments to the anomeric carbon, generating (C) β -fucosides capable of engaging both the sugar-binding site and its neighboring site.

Concerning the linker, a single “fit-all” function was not possible, as the structures, orientations, and distances to the anomeric position varied from fragment to fragment.²⁵ Instead, a set of linkers were explored, with different characteristics in terms of bridging length, angle, flexibility, bulkiness, polarity and metabolic stability. Among these, the alkyne function was particularly interesting as a connector: a β -fucosylalkyne had an appropriate orientation, acceptable length, and could be accessed through versatile chemistry. Alternatively, an amide bond was more easily synthesized and offered polar surfaces to interact with a nearby crystallographically conserved water molecule. Other linkages that seemed viable at this point for some of the fragments were a *E*-alkene bond and a 1,4-triazole ring (**Figure 1B**). To validate the design, the bifunctional ligands were screened *in silico* by docking, as described in the Supporting information (Section 2). The first generation of antagonists was thus designed as a panel of β -C- and β -N-fucoside glycomimetic bifunctional molecules, simultaneously targeting BC2L-C-Nt's carbohydrate binding site and its neighboring site (**Figure 1C**).

Modular Synthesis of β -C- and β -N-Fucosides

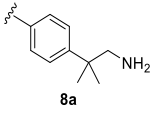
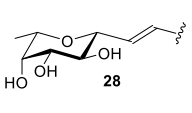
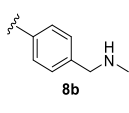
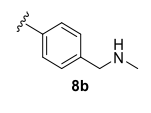

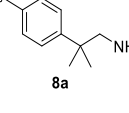
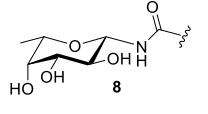
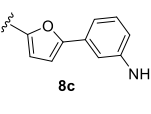
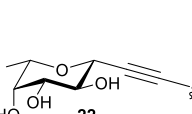
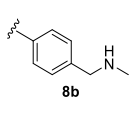
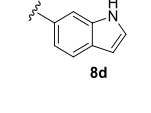

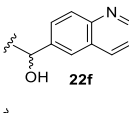
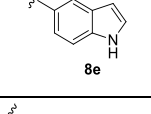

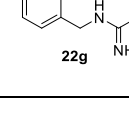
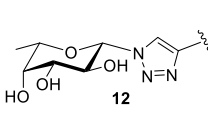
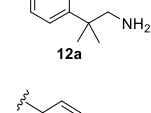
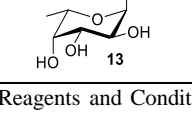
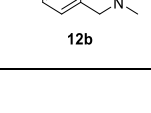
The synthetic route towards the designed fucosides was drafted to satisfy two requirements: (1) to be modular, allowing for all final molecules to be synthesized from the same building blocks; (2) to feature robust and reliable coupling procedures, in order to accommodate a range of fragment structures that could be expanded in the future. **Scheme 1** summarizes how this approach was implemented starting from fucose through two key intermediates, the β -azidofucoside **2** and the β -fucosylacetylene **3**. They could be coupled either directly or after minimal manipulation to the appropriately functionalized fragments (exemplified by **4** and its derivatives in **Scheme 1**), affording the full set of designed connections.



Scheme 1. Modular synthesis towards β -C- and β -N-Fucosides exemplified for fragment **4**.

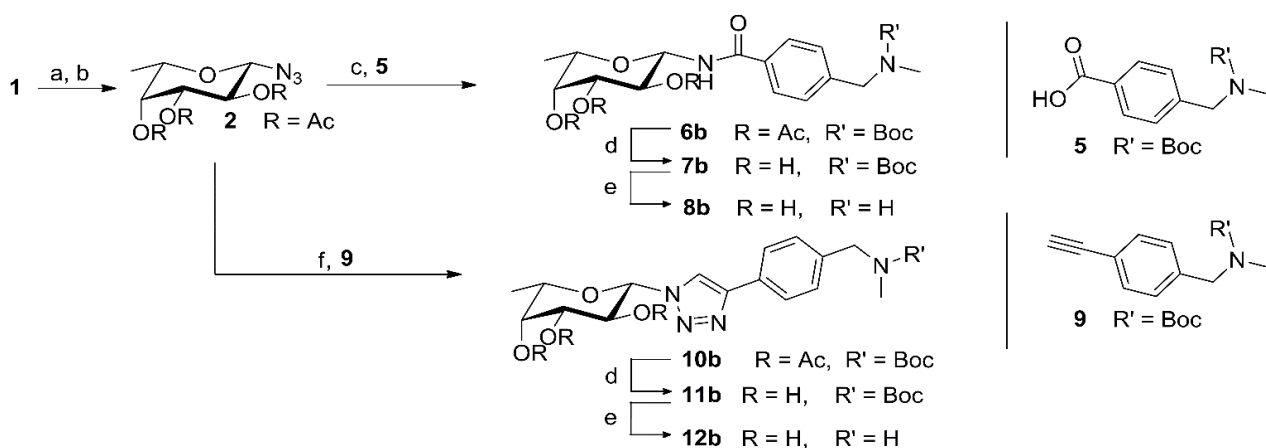
In detail, acetylation of L-fucose **1** and reaction with TMSN_3 promoted by SnCl_4 provided the azido intermediate **2** in good yields (67% over two steps) and selectivity (α/β ratio 9:91) (**Scheme 2**). Coupling of **2** with carboxylic partners, exemplified by **5** in **Scheme 2**, under Staudinger conditions, followed by protecting group removal steps as needed, led to amides **8a-e** (**Table 1**). Reaction of **2** with alkyne partners, such as **9**, under CuAAC conditions (**Scheme 2**) afforded triazole-linked bifunctional molecules that were deprotected giving **12a-b** (**Table 1**).

Table 1. Panel of β -N- and β -C-Fucosides, affinity evaluation by SPR and ITC^a

Fucoside moiety	Fragment moiety	SPR K _D [mM]	ITC K _D [mM]	Fucoside moiety	Fragment moiety	SPR K _D [mM]	ITC K _D [mM]
	 8a	0.94 ± 0.01	2.55 ± 1.00	 28	 8b	1.02 ± 0.02	3.37 ± 0.40
	 8b	1.57 ± 0.06	3.66 ± 0.21	 8a	 8a	1.33 ± 0.15	0.28 ± 0.01
 8	 8c	2.36 ± 0.97	n.d. ^b	 22	 8b	7.85 ± 3.39 ^c	1.24 ± 0.07
	 8d	3.42 ± 0.22	3.49 ± 1.30	 22f	 22f	0.301 ± 0.001	0.49 ± 0.08
	 8e	1.42 ± 0.02	0.76 ± 0.03	 22g	 22g	1.3 ± 0.6	0.91 ± 0.03
 12	 12a	1.19 ± 0.05	2.49 ± 0.06	 13	-	-	2.70 ± 0.7 ^a
	 12b	2.45 ± 0.02	6.25 ± 0.72				

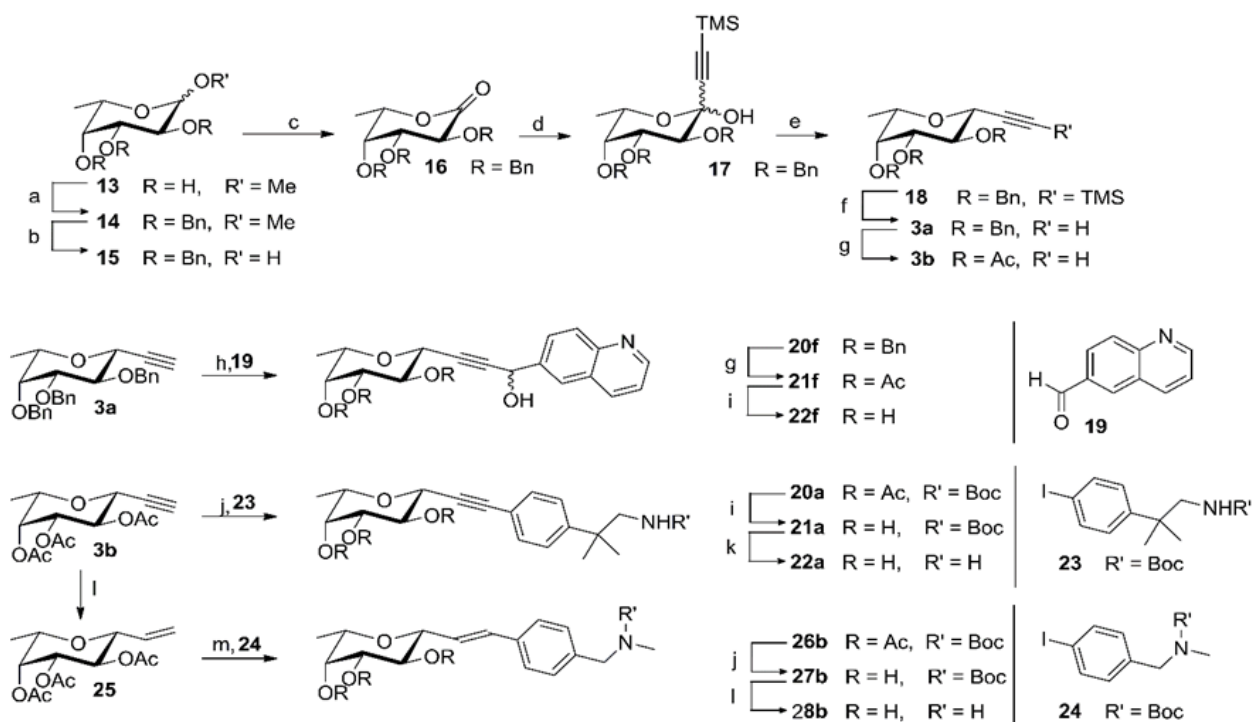
^aReagents and Conditions as shown in **Scheme 2** and **3**. ^bFrom Šulák and co-workers²² ^cObtained from **6c-e**. ^dCould not be determined, due to low solubility of **8c** ^eAspecific interaction with the chip observed ^fR = Bn ^gOver two steps (benzyl/acetate exchange and hydrolysis).

The key β -fucosylacetylene **3** was synthesized adapting a methodology established for β -galactosylacetylenes (**Scheme 3**).^{26,27} This slightly adapted route is, to the best of our knowledge, the first report of stereoselective synthesis of β -fucosylacetylene as a building block. Starting from methyl α -L-fucopyranoside **13**, a protection/deprotection scheme (**13-15** in **Scheme 3**) followed by oxidation of the anomeric carbon (I₂, 75%) led to the fuconolactone **16**. An organocerium reaction was used to install the acetylene moiety, resulting in **17** (87%) as an anomeric mixture, which was deoxygenated (Et₃SiH, BF₃•Et₂O) to afford the β -fucosyl-trimethylsilylacetylene **18** with complete stereoselectivity. TMS removal under basic conditions (NaOH) produced the terminal alkyne **3a**. A permutation of protecting groups by acetolysis provided **3b**.



Scheme 2. Synthesis of β -N-Fucosides exemplified for one fragment. Reagents and conditions: **a.** Ac_2O , Pyr, rt; **b.** TMS-N_3 , SnCl_4 , DCM, 0°C , 67% (over 2 steps); **c.** PMe_3 , DCM, rt; then: carboxylic acid **5**, HATU, DIPEA, DCM, rt, 45%; **or:** H_2 , Pd/C, MeOH, rt; then: carboxylic acid **5**, HATU, DIPEA, DCM, rt; **d.** MeONa , MeOH, rt, 83%; **or:** NH_2Me , EtOH, rt; **e.** TFA, DCM, 0°C , quant.; **f.** $\text{CuSO}_4 \cdot \text{H}_2\text{O}$, Na-Ascorbate, alkyne **9**, MeOH, rt, quant.

The *O*-benzyl intermediate **3a** was used to generate bifunctional molecules featuring a propargylic alcohol moiety. Indeed, some of the fragment screening hits bore a hydroxyl group directed towards the binding site and predicted to replace a crystallographically conserved water molecule.²⁵ Entropically speaking, successfully replacing an ordered water molecule while maintaining its interactions can translate into a considerable affinity gain. Consequently, we aimed to validate this synthetic route with at least one structure. Starting from **3a**, an organolithium reaction mediated by LDA allowed nucleophilic attack of the fucosylalkyne onto the aldehyde-bearing fragment **19**, resulting in **20f**. This reaction afforded a 1:1 mixture of stereoisomers, as observed by $^1\text{H-NMR}$ spectroscopy of the crude reaction mixture (600 MHz). Acetolysis and de-acetylation afforded the deprotected diastereomeric mixture **22f**, which could not be chromatographically resolved and was tested as such.



Scheme 3. Synthesis of β -C-Fucosides exemplified for three fragments. ^aReagents and conditions: a. BnBr, KOH, Tol, 111°C, 80%; b. HCl, AcOH, 118°C, 78%; c. I₂, K₂CO₃, DCM, rt, 75%; d. TMS-acetylene, nBuLi, CeCl₃, THF, -78°C, 87%; e. Et₃SiH, BF₃·Et₂O, CH₃CN/DCM, -10°C, 86%; f. NaOH, MeOH/DCM, rt, 99%; g. TMSOTf, Ac₂O, rt, 61%. h. LDA, aldehyde 19, THF, -20°C, 72%; i. MeONa, MeOH, rt; j. Sonogashira: Pd(PPh₃)₄, CuI, fragment 23, Piperidine, 80°C; k. TFA, DCM, 0°C; l. Lindlar's Pd catalyst, H₂, MeOH, 89%; m. Heck: Pd(OAc)₂, KCl, TBAB, K₂CO₃, AgNO₃, fragment 24, DMF, 100 °C, 81%. Omitted yields are reported in SI Table S3.

The alkyne **3b** was used for Sonogashira coupling with iodinated fragments, as exemplified by **23** and **24** in **Scheme 3** to afford alkynes **20a** and **20b** in yields over 80%. Subsequent deprotections led to bifunctional ligands **22a** and **22b** (see **Table 1**). The guanidine containing ligand **22g** (**Table 1**) was obtained by Goodman guanidinylation of **20b**,²⁸ as described in the Supporting information. Additionally, **3b** was transformed in the corresponding alkene **25** (Lindlar's Pd catalyst), which underwent Heck coupling (Pd(OAc)₂, KCl, TBAB, K₂CO₃, AgNO₃, DMF, 100 °C) with **24**, to selectively afford the *E*-product **26b**. Subsequent deprotections afforded the final alkene **28b** (**Table 1**).

To recap, synthetic routes towards the β -fucosylazide **2** and the β -fucosylacetylene **3** intermediates were validated. Coupling these intermediates to appropriately functionalized fragments led to four families of *N*- or *C*-fucosides. Thus, a modular synthesis framework allowing for rapid and stereoselective synthesis of β -*C*- and β -*N*-fucosides was drafted and validated, resulting in a panel of potential BC2L-C-Nt ligands to be screened against the protein target. **Table 1** collects the

molecules synthesized through this framework: amides **8a-e**, triazoles **12a-b**, alkynes **22a,b,f,g** and alkene **28b**.

The remaining part of the work involved the synthesis of the functionalized fragments, which is detailed in the Supporting information (Section 1.3).

Biophysical Evaluation of the Glycomimetics

In order to evaluate the affinity of the newly synthesized structures for their target BC2L-C-Nt, Surface Plasmon Resonance (SPR) and Isothermal Titration Calorimetry (ITC) were employed. SPR evaluation of the synthetic structures against a BC2L-C-Nt -coated chip resulted in low millimolar affinities (Table 1, Figure 2A and B). These values are comparable with the affinity established for α MeFuc (ITC: 2.7 mM).²² With K_D values in the range of [0.3 - 3.4 mM], most ligands could be considered equivalent. Nevertheless, some of the better-performing compounds on SPR produced key results in ITC (22a, 22f-g) or crystallography (8c). Additional limitations in the SPR experiments included the non-specific interactions observed between molecule 22b and the chip, which explains the outlying affinity recorded (7.85 mM). Moreover, a degree of variability was observed for the values measured on different protein chips. Thus, SPR allowed for a material-economic early ligand screening, resulting in a preliminary ranking of structures and in the identification of outliers and potential hits, fit for further assaying with different techniques.

ITC evaluation returned K_D values spread in a wider range than SPR: [0.28 – 6.25 mM]. This allowed a better sense of which compounds performed worse than the natural monosaccharide, and which could become hits (**Table 1**). Of the evaluated panel, one amide (**8e**) and all four alkynes (**22a-g**) displayed a better activity than methyl-fucoside **13**. In particular, alkyne **22f** with a K_D of 490 μ M confirmed the good affinity observed by SPR. However, this molecule was tested as a mixture of unseparable stereoisomers and further studies are required to obtain a stereoselective synthesis and assess the activity of the single epimers. Alternatively, **22a** with a K_D of 281 μ M was identified as the main hit with suitable values in both SPR and ITC (see **Figure 2C**) and a nearly 10-fold affinity increase from α MeFuc. Importantly, this simple ligand is also only one order of magnitude less active than the Globo H hexasaccharide (Fuc α 1-2Gal β 1-3GalNAc β 1-3Gal α 1-4Gal β 1-4Glc), which is the strongest known natural ligand of BC2L-C-Nt.²² This promising result validates the ligand design by fragment screening, as well as the choice of the acetylene moiety as a linker. Finally, the very low solubility of amide **8c** prevented affinity evaluation by ITC. However, both **22a** and **8c** went on to provide crystal structures in complex with the protein (see following section).

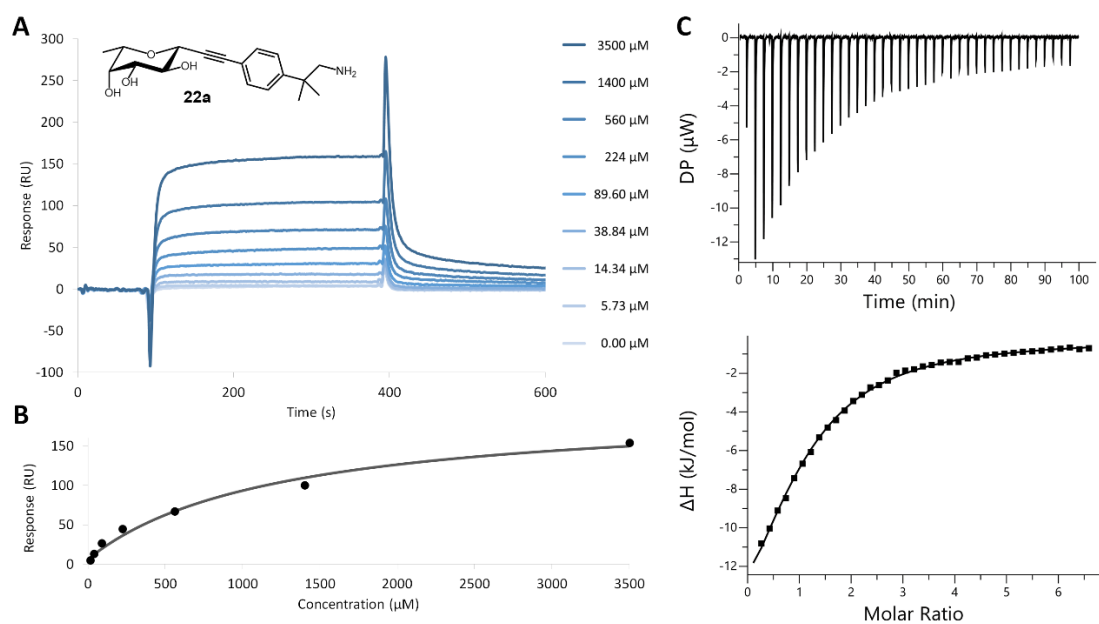


Figure 2. ITC and SPR experiments: (A, B) SPR analysis of **22a** binding to BC2L-C-Nt, multi-cycle sensogram and affinity analysis. (C) ITC titration of BC2L-C-Nt by **22a** (stoichiometry fitted to $N = 1$).

Saturation Transfer Difference NMR (STD-NMR) experiments allowed us to further characterize the interaction between BC2L-C-Nt and hit **22a** (Figure 3). Two STD experiments were performed, irradiating either aliphatic (-0.05 ppm, Figure 3B) or aromatic (10 ppm, Figure 3C) residues of the protein. The ligand protons close to the directly irradiated protein protons could thus be revealed by a relative increase in STD intensities. Irradiation of the aliphatic residues (Figure 3B) resulted in strong signals for the methyl group in position 6 of the fucoside (1.26 ppm), indicating close contact to the protein, as observed for the monosaccharide in earlier work.²⁵ Weaker STD signals were also observed for the H2 of the fucoside ring (3.74 ppm) and the aromatic signals of the fragment moiety (7.44, 7.52 ppm). On the other hand, irradiation at 10 ppm (Figure 3C) produced an STD signal only for the aromatic protons of the ligand, hinting at a close contact to aromatic residues of the protein.

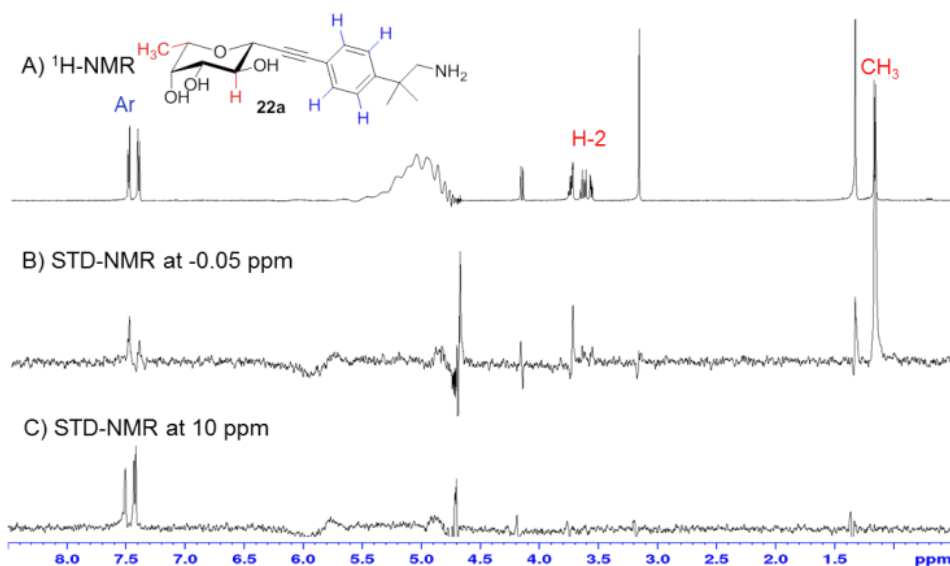


Figure 3. $^1\text{H-NMR}$ (A) and Saturation Transfer Difference NMR experiments for **22a**, acquired using -0.05 ppm (for the irradiation of the aliphatic residues of the protein, B) and 10 ppm (for the irradiation of aromatic amino acids, C). The signals of aromatic protons are highlighted in blue, the protons of fucose in red.

These results confirmed that **22a** adopts the known fucoside binding mode, in which the main protons exposed to the protein belong to C2 and C6. This, added to the aromatic signals observed for the fragment moiety, support the expected binding mode of the ligand as designed, which was indeed later confirmed crystallographically (see below, **Figure 5**).

Since both the fucoside binding site and its vicinal site are located at the interface between monomers, it was interesting to evaluate the effect of the binding event on protein stability. For this, Differential Scanning Calorimetry (DSC) experiments were performed. First, a reference experiment allowed to define the protein's unfolding profile upon a rising temperature gradient (**Figure 4A**). The data obtained suggested two sequential thermal events, T_{m1} and T_{m2} , which could be attributed to the separation of monomers followed by their unfolding. The melting temperatures recorded were $T_{m1} = 82.2\text{ }^\circ\text{C}$ and $T_{m2} = 84.5\text{ }^\circ\text{C}$. The addition of ligands to the protein could either increase (stabilizing) or decrease (destabilizing) these melting temperatures. Although stabilization of the protein is usually observed for complexes, destabilization would be observed if the synthetic ligand **22a** disrupts the protomeric interface. For comparison, the same experiment was performed for a known oligosaccharide ligand, the H-type 1 trisaccharide ($\text{Fuc}\alpha(1-2)\text{Gal}\beta(1-3)\text{GlcNAc}$), which binds to BC2L-C-Nt with micromolar affinity.²⁴ The results obtained are summarized in **Figure 4**. As predicted for a stabilized complex, the H-type 1 trisaccharide provided a positive ΔT_m values of $+0.4\text{ }^\circ\text{C}$ for each of the events (**Figure 4B**). To a lesser degree, synthetic ligand **22a** similarly stabilized the protein with a ΔT_m value of $+0.2\text{ }^\circ\text{C}$ for both events.

These results confirm no detrimental effect to the stability of the BC2L-C-Nt trimer by either type of ligand.

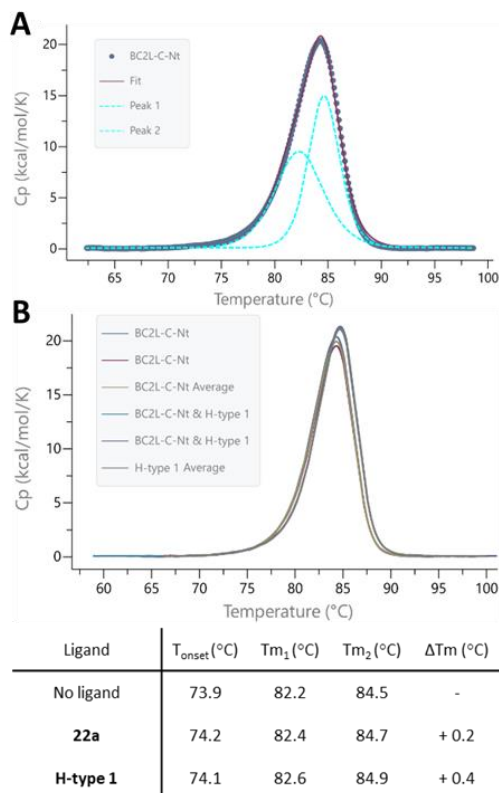


Figure 4. Differential Scanning Calorimetry: (A) Fitting with two thermal events. (B) Representative experiment comparing presence and absence of ligand H-type 1.

Structures of BC2L-C-Nt in Complex with Antagonists

We solved two new crystal structures featuring complexes of BC2L-C-Nt with synthetic ligands **22a** and **8c**, allowing further rationalization of the affinity observed. The structures resulted from soaking BC2L-C-Nt crystals for 24 h in a 1.25 mM solution of each ligand and were solved to 1.79 Å and 1.32 Å resolution by molecular replacement. The relevant statistics can be found in the Supporting Information (Section 3, **Table S4**). Inspection of the protein/ligand interactions as seen in **Figure 5** confirmed the known fucoside binding mode from prior crystal structures: in both complexes the sugar moiety establishes H-bonds with residues Thr74, Thr83, Arg85 and Arg111, as well as water-mediated contacts with Tyr75, Ser82, and Tyr58 (crystallographic waters **W1** and **W2**, respectively). A hydrophobic interaction between the C6 methyl group of the fucose moiety and the aromatic ring of Tyr48 is also observed.^{22,24}

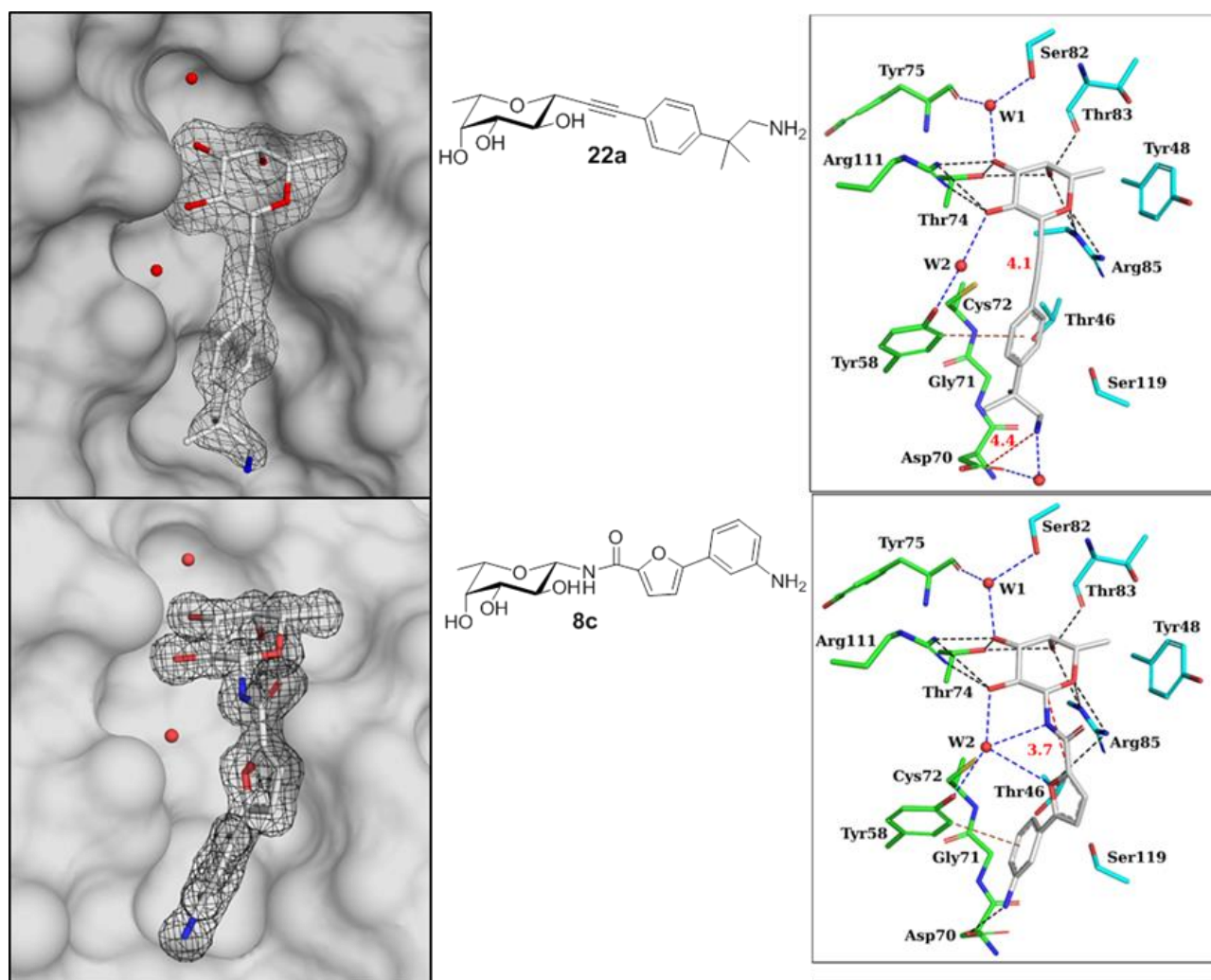


Figure 5. Left: Electronic density for synthetic ligands **22a** (top, 1.79 Å) and **8c** (bottom, 1.32 Å) in complex with BC2L-C-Nt. Water molecules **W1** and **W2** are depicted as red spheres, protein surface in transparent gray. Right: Deposited crystal structures (PDB: 7OLU, top and 7OLW, bottom). Direct protein/ligand interactions are shown in black (hydrophobic) or brown (edge-to-face π/π); water-mediated contacts are shown in blue. Distances (Å) from anomeric carbon to fragment or from amino group to Asp70 are depicted in red.

In the structure featuring ligand **22a**, the alkyne linker is 4.1 Å-long and does not significantly dislocate the nearby crystallographic water **2** (**Figure 5**, top). The fragment's aromatic moiety engages in the predicted π/π T-shaped interaction with Tyr58, with an edge-to-face distance of 3.9 Å between its centroid and the closest C-atom of Tyr58 side chain, albeit the angle is 58°, rather than 90° (**Figure 5**, top). Lastly, the salt bridge between amino group and Asp70 carboxyl side chain predicted in the docked pose of the corresponding fragment (Supporting information, Section 2, **Figure S2B**) is not observed, possibly because the alkyne linker is shorter than the optimal fucose-fragment distance suggested by docking (4.1 Å vs. 4.9 Å). Nevertheless, a water-mediated contact between these groups is observed. Other characteristics of this interaction includes the shape

complementarity of hydrophobic patches: both methyl groups of the fragment are in close proximity with the otherwise exposed hydrophobic surface generated by the main chain of Gly71 and side chain of Tyr58. This hydrophobic complementarity carries on to match with residues Cys72, Thr46 and Ser119.

In the complex with ligand **8c**, the ligand features an amide linker, positioning the fragment moiety 3.7 Å away from the anomeric carbon (**Figure 5**, bottom). Designed to either replace or interact with crystallographic water **2**, the amide bond interacts through its nitrogen atom, while the carbonyl points towards the solvent. The experimental structure perfectly matches the previously generated docking pose, including a π/π T-shaped interaction with Tyr58 (3.6 Å) and H-bonding interactions between water **2** and the furan moiety, as well as between the side chain of Asp70 and the aniline moiety (Supporting Information, Section 2, **Figure S3**). In terms of shape complementarity, this ligand is more solvent exposed than the former, except for its aniline moiety, which matches the aforementioned hydrophobic patch composed of Gly71, Tyr58 and Thr46.

It is worth noting that in previous BC2L-C-Nt structures, at least two water molecules consistently resided in the space now filled by the fragment moieties. This displacement of ordered water can translate into entropic gains, especially since the water molecules in question did not establish consistent and conserved interactions with their surroundings. Altogether, the data presented confirm the compatibility of β -oriented substituents and the known fucoside binding mode. The alkyne and amide linkers are appropriate for this design. The structures also validate the binding poses predicted for the ligand or fragment structures (Supporting Information, Section3, **Figures S2** and **S3**), with the length of the linker being a limit for the latter. Additionally, we can rationalize the affinity gain observed for hit structure **22a** as the result of three factors: (1) the T-shaped π/π interaction, (2) the shape complementarity between hydrophobic surfaces, and (3) the thermodynamically advantageous entropic factor. Finally, the results with structure **8c** motivates the need to modulate its poor solubility in a future second generation design.

▪ CONCLUSIONS

We have developed a campaign of characterization and probing of a new biological target: the *superlectin* BC2L-C from *Burkholderia cenocepacia*. We have focused on the study of its N-terminal lectin domain and of the carbohydrate binding site it features. With the acquired data, we

have designed the first generation of antagonists for this lectin, which consist of bifunctional β -C- or β -N-fucosides. Each of these bifunctional molecules bears a fragment moiety selected by *in silico* screening and aims to simultaneously targeting the sugar binding site and a vicinal region at the interface of two protomers. To ensure access to the designed structures, we conceived and validated a modular synthetic framework which allows the straightforward synthesis of both β -N- and β -C-fucosides and can be widely applied for the synthesis of amide-, triazole-, alkyne- and alkene-bound glycomimetics. Thus, we generated a panel of BC2L-C-Nt antagonists. The synthesized molecules were probed against their target by a range of techniques. In particular, STD-NMR and DSC showed definite although moderate responses and we envision their potential to serve as early screens for future generations of antagonists. Finally, ITC allowed us to unambiguously claim two successful hits with improved affinity compared to the monosaccharide parent structure. The current leading antagonist **22a** presented a 10-fold affinity gain and validated our strategy, as well as the use of alkyne linkers in glycomimetic ligand design. In this context, it is important to stress that, while no general strategies exist for the rational design of glycomimetic lectin ligands, many of the reported hits contain a natural monosaccharide, meant to act as an anchor and to direct the ligand to the lectin carbohydrate recognition domain. Supplementary fragments capable of establishing additional interactions with the protein target in the vicinity of the carbohydrate binding site are then connected to the sugar core, possibly using non-glycosidic linkages. The nature of these fragments is often defined by trial and error. The work we report here shows that virtual screening of fragment libraries in the lectin complex of monosaccharides is an appropriate tool for fragment selection and rational design of glycomimetic structures.

Finally, we have solved the first crystal structures of BC2L-C-Nt complexes with synthetic ligands, validating our computational and experimental work so far, as well as the choice of amide linkers. Altogether, this successful campaign has opened the way to drugging BC2L-C. On one hand, a clear synthetic avenue leads to a class of validated antagonist structures. On the other hand, the campaign has allowed for preliminary SAR, which will be useful for the design of a second generation of antagonists.

▪ ASSOCIATED CONTENT

Supporting Information

Experimental procedures, ^1H and ^{13}C NMR spectra and characterization of the compounds, data collection and refinement statistics are available free of charge at <http://pubs.acs.org>; structure coordinates, structure factors, as well as validation reports can be downloaded from PDB website at <https://www.rcsb.org> (PDB code 7OLU and 7OLW).

▪ AUTHOR INFORMATION

Corresponding Authors

Anna Bernardi - *Università degli Studi di Milano, Dipartimento di Chimica, via Golgi 19, 20133 Milano, Italy*, <https://orcid.org/0000-0002-1258-2007>, anna.bernardi@unimi.it

Annabelle Varrot - *Univ. Grenoble Alpes, CNRS, CERMAV, 38000 Grenoble, France*, <https://orcid.org/0000-0001-6667-8162>, annabelle.varrot@cermav.cnrs.fr

Authors

Rafael Bermeo - *Università degli Studi di Milano, Dipartimento di Chimica, Milano, Italy; Univ. Grenoble Alpes, Grenoble, France*

Kanhaya Lal - *Università degli Studi di Milano, Dipartimento di Chimica, Milano, Italy; Univ. Grenoble Alpes, Grenoble, France*

Davide Ruggeri - *Università degli Studi di Milano, Dipartimento di Chimica, Milano, Italy; Present address: Department of Chemistry, Life Sciences and Environmental Sustainability, University of Parma, Parma, Italy*

Daniele Lanaro - *Università degli Studi di Milano, Dipartimento di Chimica, Milano, Italy*

Sarah Mazzotta - *Università degli Studi di Milano, Dipartimento di Chimica, Milano, Italy*

Francesca Vasile - *Università degli Studi di Milano, Dipartimento di Chimica, Milano, Italy*

Anne Imberty - *Univ. Grenoble Alpes, CNRS, CERMAV, Grenoble, France*

Laura Belvisi - *Università degli Studi di Milano, Dipartimento di Chimica, Milano, Italy*

Notes

The authors declare no competing financial interest.

▪ ACKNOWLEDGMENTS

This research was funded by the European Union's Horizon 2020 research and innovation program under the Marie Skłodowska-Curie grant agreement No 765581 (PhD4GlycoDrug). AI and AV are partially supported by Glyco@Alps (ANR-15-IDEX-02) and Labex Arcane/CBH- EUR-GS (ANR-17-EURE-0003). We are grateful to Valérie Chazalet, Emilie Gillon and Sue Kuhaudomlarp for lab support (CERMAV). We thank also Olivier Renaudet for logistical assistance (DCM, Grenoble). Crystal data collection was performed at the SOLEIL Synchrotron, Saint Aubin, France (proposal 20191314), we are grateful for access and technical support by Pierre Montaville, Martin Savko and William Shepard at beamlines Proxima 1 and 2.

▪ REFERENCES

- (1) Essack, S. Water, Sanitation and Hygiene in National Action Plans for Antimicrobial Resistance. *Bull. World Health Organ.* **2021**, *99* (8), 606–608. <https://doi.org/10.2471/BLT.20.284232>.
- (2) Serra-Burriel, M.; Keys, M.; Campillo-Artero, C.; Agodi, A.; Barchitta, M.; Gikas, A.; Palos, C.; López-Casasnovas, G. Impact of Multi-Drug Resistant Bacteria on Economic and Clinical Outcomes of Healthcare-Associated Infections in Adults: Systematic Review and Meta-Analysis. *PLoS One* **2020**, *15* (1), 0227139. <https://doi.org/10.1371/journal.pone.0227139>.
- (3) Garcia-Clemente, M.; de la Rosa, D.; Máiz, L.; Girón, R.; Blanco, M.; Oliveira, C.; Canton, R.; Martínez-García, M. A. Impact of Pseudomonas Aeruginosa Infection on Patients with Chronic Inflammatory Airway Diseases. *J. Clin. Med.* **2020**, *9* (12), 9123800. <https://doi.org/10.3390/jcm9123800>.
- (4) Mahenthiralingam, E.; Urban, T. A.; Goldberg, J. B. The Multifarious, Multireplicon Burkholderia Cepacia Complex. *Nat. Rev. Microbiol.* **2005**, *3* (2), 144–156. <https://doi.org/10.1038/nrmicro1085>.
- (5) Krachler, A. M.; Orth, K. Targeting the Bacteria-Host Interface Strategies in Anti-Adhesion Therapy. *Virulence* **2013**, *4* (4), 284–294. <https://doi.org/10.4161/viru.24606>.
- (6) Heggelund, J. E.; Varrot, A.; Imberty, A.; Kregel, U. Histo-Blood Group Antigens as Mediators of Infections. *Curr. Opin. Struct. Biol.* **2017**, *44*, 190–200. <https://doi.org/10.1016/j.sbi.2017.04.001>.
- (7) Cozens, D.; Read, R. C. Anti-Adhesion Methods as Novel Therapeutics for Bacterial Infections. *Expert Rev. Anti. Infect. Ther.* **2012**, *10* (12), 1457–1468. <https://doi.org/https://doi.org/10.1586/eri.12.145>.
- (8) Hatton, N. E.; Baumann, C. G.; Fascione, M. A. Developments in Mannose-Based Treatments for Uropathogenic Escherichia Coli-Induced Urinary Tract Infections. *ChemBioChem* **2021**, *22* (4), 613–629. <https://doi.org/10.1002/cbic.202000406>.

- (9) Sattin, S.; Bernardi, A. Glycoconjugates and Glycomimetics as Microbial Anti-Adhesives. *Trends Biotechnol.* **2016**, *34* (6), 483–495. <https://doi.org/10.1016/j.tibtech.2016.01.004>.
- (10) Calvert, M. B.; Jumde, V. R.; Titz, A. Pathoblockers or Antivirulence Drugs as a New Option for the Treatment of Bacterial Infections. *Beilstein J. Org. Chem.* **2018**, *14*, 2607–2617. <https://doi.org/10.3762/bjoc.14.239>.
- (11) Meiers, J.; Siebs, E.; Zahorska, E.; Titz, A. Lectin Antagonists in Infection, Immunity, and Inflammation. *Curr. Opin. Chem. Biol.* **2019**, *53*, 51–67. <https://doi.org/10.1016/j.cbpa.2019.07.005>.
- (12) Tamburrini, A.; Colombo, C.; Bernardi, A. Design and Synthesis of Glycomimetics: Recent Advances. *Med. Res. Rev.* **2020**, *40* (2), 495–531. <https://doi.org/10.1002/med.21625>.
- (13) Bernardi, A.; Sattin, S. Interfering with the Sugar Code: Ten Years Later. *European J. Org. Chem.* **2020**, *2020* (30), 4652–4663. <https://doi.org/10.1002/ejoc.202000155>.
- (14) Mitchell, E.; Houles, C.; Sudakevitz, D.; Wimmerova, M.; Gautier, C.; Pérez, S.; Wu, A. M.; Gilboa-Garber, N.; Imberty, A. Structural Basis for Oligosaccharide-Mediated Adhesion of *Pseudomonas Aeruginosa* in the Lungs of Cystic Fibrosis Patients. *Nat. Struct. Biol.* **2002**, *9* (12), 918–921. <https://doi.org/10.1038/nsb865>.
- (15) Johansson, E. M. V.; Cruz, S. A.; Kolomiets, E.; Buts, L.; Kadam, R. U.; Cacciarini, M.; Bartels, K. M.; Diggle, S. P.; Cámara, M.; Williams, P.; Loris, R.; Nativi, C.; Rosenau, F.; Jaeger, K. E.; Darbre, T.; Reymond, J. L. Inhibition and Dispersion of *Pseudomonas Aeruginosa* Biofilms by Glycopeptide Dendrimers Targeting the Fucose-Specific Lectin LecB. *Chem. Biol.* **2008**, *15* (12), 1249–1257. <https://doi.org/10.1016/j.chembiol.2008.10.009>.
- (16) Gustke, H.; Kleene, R.; Loers, G.; Nehmann, N.; Jaehne, M.; Bartels, K. M.; Jaeger, K. E.; Schachner, M.; Schumacher, U. Inhibition of the Bacterial Lectins of *Pseudomonas Aeruginosa* with Monosaccharides and Peptides. *Eur. J. Clin. Microbiol. Infect. Dis.* **2012**, *31* (2), 207–215. <https://doi.org/10.1007/s10096-011-1295-x>.
- (17) Passos da Silva, D.; Matwichuk, M. L.; Townsend, D. O.; Reichhardt, C.; Lamba, D.; Wozniak, D. J.; Parsek, M. R. The *Pseudomonas Aeruginosa* Lectin LecB Binds to the Exopolysaccharide Psl and Stabilizes the Biofilm Matrix. *Nat. Commun.* **2019**, *10* (1), 2183. <https://doi.org/10.1038/s41467-019-10201-4>.
- (18) Sommer, R.; Rox, K.; Wagner, S.; Hauck, D.; Henrikus, S. S.; Newsad, S.; Arnold, T.; Ryckmans, T.; Brönstrup, M.; Imberty, A.; Varrot, A.; Hartmann, R. W.; Titz, A. Anti-Biofilm Agents against *Pseudomonas Aeruginosa*: A Structure-Activity Relationship Study of C-Glycosidic LecB Inhibitors. *J. Med. Chem.* **2019**, *62* (20), 9201–9216. <https://doi.org/10.1021/acs.jmedchem.9b01120>.
- (19) Lameignere, E.; Malinovská, L.; Sláviková, M.; Duchaud, E.; Mitchell, E. P.; Varrot, A.; Šedo, O.; Imberty, A.; Wimmerová, M. Structural Basis for Mannose Recognition by a Lectin from Opportunistic Bacteria *Burkholderia Cenocepacia*. *Biochem. J.* **2008**, *411* (2), 307–318. <https://doi.org/10.1042/BJ20071276>.
- (20) Šulák, O.; Cioci, G.; Lameignère, E.; Balloy, V.; Round, A.; Gutsche, I.; Malinovská, L.; Chignard, M.; Kosma, P.; Aubert, D. F.; Marolda, C. L.; Valvano, M. A.; Wimmerová, M.; Imberty, A. *Burkholderia Cenocepacia* Bc21-c Is a Super Lectin with Dual Specificity and Proinflammatory Activity. *PLoS Pathog.* **2011**, *7* (9). <https://doi.org/10.1371/journal.ppat.1002238>.

- (21) Lameignère E., PhD Thesis, Univ. Grenoble Alpes, 2009.
- (22) Šulák, O.; Cioci, G.; Delia, M.; Lahmann, M.; Varrot, A.; Imberty, A.; Wimmerová, M. A TNF-like Trimeric Lectin Domain from Burkholderia Cenocepacia with Specificity for Fucosylated Human Histo-Blood Group Antigens. *Structure* **2010**, *18* (1), 59–72. <https://doi.org/10.1016/j.str.2009.10.021>.
- (23) Sommer, R.; Wagner, S.; Rox, K.; Varrot, A.; Hauck, D.; Wamhoff, E. C.; Schreiber, J.; Ryckmans, T.; Brunner, T.; Rademacher, C.; Hartmann, R. W.; Brönstrup, M.; Imberty, A.; Titz, A. Glycomimetic, Orally Bioavailable LecB Inhibitors Block Biofilm Formation of Pseudomonas Aeruginosa. *J. Am. Chem. Soc.* **2018**, *140* (7), 2537–2545. <https://doi.org/10.1021/jacs.7b11133>.
- (24) Bermeo, R.; Bernardi, A.; Varrot, A. BC2L-C N-Terminal Lectin Domain Complexed with Histo Blood Group Oligosaccharides Provides New Structural Information. *Molecules* **2020**, *25* (2), 248. <https://doi.org/10.3390/molecules25020248>.
- (25) Lal, K.; Bermeo, R.; Cramer, J.; Vasile, F.; Ernst, B.; Imberty, A.; Bernardi, A.; Varrot, A.; Belvisi, L. Prediction and Validation of a Druggable Site on Virulence Factor of Drug Resistant Burkholderia Cenocepacia. *Chem. - Eur. J.* **2021**, *27*, 10341–10348. <https://doi.org/10.1002/chem.202100252>.
- (26) Alzeer, J.; Vasella, A. Oligosaccharide Analogues of Polysaccharides. Part 2. Regioselective Deprotection of Monosaccharide-derived Monomers and Dimers. *Helv. Chim. Acta* **1995**, *78* (1), 177–193. <https://doi.org/10.1002/hlca.19950780117>.
- (27) Lowary, T.; Meldal, M.; Helmboldt, A.; Vasella, A.; Bock, K. Novel Type of Rigid C-Linked Glycosylacetylene-Phenylalanine Building Blocks for Combinatorial Synthesis of C-Linked Glycopeptides. *J. Org. Chem.* **1998**, *63* (26), 9657–9668. <https://doi.org/10.1021/jo980517h>.
- (28) Feichtinger, K.; Zapf, C.; Sings, H. L.; Goodman, M. Diprotected Triflylguanidines: A New Class of Guanidinylation Reagents. *J. Org. Chem.* **1998**, *63* (12), 3804–3805.

